

## Investigation of Ultrafast Laser-Driven Radiative Blast Waves

M. J. Edwards,<sup>1</sup> A. J. MacKinnon,<sup>1</sup> J. Zweiback,<sup>1</sup> K. Shigemori,<sup>2</sup> D. Ryutov,<sup>1</sup> A. M. Rubenchik,<sup>3</sup> K. A. Keilty,<sup>4</sup>  
E. Liang,<sup>4</sup> B. A. Remington,<sup>1</sup> and T. Ditmire<sup>1,\*</sup>

<sup>1</sup>*Lawrence Livermore National Laboratory, Livermore, California 94550*

<sup>2</sup>*Institute of Laser Engineering, Osaka University, Suita, Osaka, 565-0871, Japan*

<sup>3</sup>*Department of Applied Science, University of California, Davis, California 95616*

<sup>4</sup>*Department of Space Physics and Astronomy, Rice University, Houston, Texas 77005*

(Received 23 October 2000; published 2 August 2001)

We have examined the evolution of cylindrically symmetric blast waves produced by the deposition of femtosecond laser pulses in gas jets. In high- $Z$  gases radiative effects become important. We observe the production of an ionization precursor ahead of the shock front and deceleration parameters below the adiabatic value of  $\frac{1}{2}$  (for a cylinder), an effect expected when the blast wave loses energy by radiative cooling. Despite significant radiative cooling, the blast waves do not appear to develop thin shell instabilities expected for strongly radiative waves. This is believed to be due to the stabilizing effect of a relatively thick blast wave shell resulting in part from electron thermal conduction effects.

DOI: 10.1103/PhysRevLett.87.085004

PACS numbers: 52.50.Jm, 52.35.Tc, 52.70.-m, 96.50.Fm

Astrophysical shocks play an important role in the evolution of the interstellar medium (ISM) providing an energy source and triggering a variety of phenomena including star formation [1]. On galactic time scales, supernovae are a frequent source of such shock waves, which expand into the surrounding ISM sweeping up material into a thin, dense shell. If the circumstellar medium is sufficiently dense, radiation transport can play an important role in the evolution of the supernova remnant blast wave [2,3]. Theoretical simulations indicate that strongly radiative scenarios lead to a number of consequences; these include the production of a UV driven ionization front ahead of the blast wave [4] and a blast wave front deceleration greater than a simple adiabatic blast wave due to energy depletion by radiative cooling [2]. These effects are believed to have important consequences on the evolution of supernova remnants and the complex structure observed around many of them [5].

A blast wave is often characterized by its asymptotic trajectory  $R(t) = \beta t^\alpha$ , where the deceleration parameter  $\alpha = Vt/R$ . Here  $V$  and  $R$  are, respectively, the velocity and the radius of the shock wave at time  $t$  after the explosion. Much can be learned from  $\alpha$ . For example, the classical spherical energy conserving Sedov-Taylor wave consisting of a high pressure low density central core pushing a thin compressed shell has  $\alpha = \frac{2}{5}$  [6] (while  $\alpha = \frac{1}{2}$  for cylindrically symmetric waves). If the surrounding gas is sufficiently dense, radiative cooling is expected to be important and the deceleration parameter falls below the Sedov-Taylor value, approaching  $\alpha = \frac{2}{7}$  which is the theoretically predicted parameter once the age of the remnant exceeds the radiative cooling time of the shell. In this so-called “pressure driven snowplow” regime the low density central core continues to exert pressure on a shell which can no longer support itself and which then collapses to high density. During the transition to this phase a host of hydrodynamic instabilities have been predicted

such as Vishniac’s overstability [7]. If radiative cooling of the hot low density core is also efficient, the pressure of the core becomes negligible, and the wave enters the “momentum conserving snowplow” regime, in which  $\alpha = \frac{1}{4}$  ( $\alpha = \frac{1}{3}$  for the cylindrical case). In this limit, the thin shell simply coasts into the surrounding gas and slows as it accretes mass.

Because of the complicated dynamics associated with these astrophysical phenomena, there is a strong motivation to produce radiative blast waves in the laboratory. A radiative blast wave can occur over a wide range of temperatures and densities in astrophysical shocks but is more difficult to achieve in the laboratory [8]. Nonetheless, high Mach number, laser driven blast waves in certain dense gases can reach the high temperatures needed to enter the radiative regime [9]. Previously, Grun *et al.* reported experiments on laser driven spherical blast waves in nitrogen and xenon [10]. Though these experiments observed blast wave trajectories that appeared consistent with a purely energy conserving (adiabatic) trajectory, they did observe the growth of Vishniac-type thin shell instabilities in xenon blast waves. This was attributed to the large compressions associated with radiative cooling.

To produce a laser driven radiative blast wave we utilized the now well characterized high absorption efficiency of high intensity femtosecond lasers in gases containing large clusters [11,12]. An intense laser focused into a strongly absorbing cluster gas produces a hot, elongated filament which subsequently develops into a cylindrical shock [13]. In this Letter, we report on experimental studies of cylindrically symmetric blast waves produced in gas jets of neon, argon, and xenon. We find that in xenon, we can produce blast waves that exhibit not only the predicted UV ionization precursor but also the increased deceleration predicted when a blast wave loses a substantial fraction of its initial energy through radiation. However, we do not observe the

growth of thin shell instabilities expected in this strongly radiative regime.

The blast waves were produced in the laboratory by focusing 0.1 J, 35 fs laser pulses with an  $f/15$  lens into a gas jet expelling a plume of neon, argon, or xenon gas. The gas jet was a sonic nozzle with a 0.5 mm diameter aperture. The laser was focused along an axis perpendicular to the gas jet axis, roughly 7 mm below the jet nozzle aperture. The interferometry described below showed that the gas density was uniform to  $<10\%$  over 1 mm, the maximum extent of the blast wave propagation in our experiments. We have therefore assumed in the data analysis that the background gas density is uniform as the blast wave propagates. Our focusing geometry resulted in a cylindrical plasma filament  $\sim 50 \mu\text{m}$  in diameter stretching across the 4 mm width (full width at half maximum) of the gas jet. In argon and xenon gas jets, clusters form and a large fraction of the laser energy was absorbed by the gas (50%), and roughly 10 mJ of energy deposited per mm, which is enough to heat the plasma filament to  $\sim 100$  eV. No clusters form in the neon gas jet and the absorption efficiency is substantially lower [12]; in this case only  $\sim 1$  mJ of energy was deposited per mm. The gas density in which the subsequent blast wave evolves could be controlled by varying the gas jet backing pressure and could be changed from about  $10^{18}$  to  $10^{19}$  atoms/cm $^3$ .

The evolution of the blast wave in the gas was probed by splitting a small portion of the laser energy and passing it perpendicularly across the plasma filament. Two techniques were used to examine the blast wave. The filament probed with the laser pulse was imaged with magnification [ $\times(2-4)$ ] into a shearing Michelson interferometer. Light traversing the plasma interfered with light passing below the plasma. Assuming cylindrical symmetry, an Abel inversion was performed on the observed phase shift to retrieve the electron density as a function of radius (with a spatial resolution of  $5-10 \mu\text{m}$ ). Varying the delay of the probe with respect to the pump pulse on successive shots permitted mapping of the electron density (and thus the shock front) evolution as a function of time. In addition, we examined the blast waves by removing the interferometer and simply imaging the plasma onto the CCD detector when a small, wire stop was placed at the focal plane of the imaging telescope. This “dark field” imaging technique provides information on the spatial derivative of the electron density and is particularly sensitive to modulations on the blast wave front and, hence, instability growth.

From the interferograms, we see the clear formation of a blast wave by 4–6 ns in most cases. Characteristic interferograms and deconvolved electron density profiles of blast waves produced in neon, argon, and xenon are illustrated in Fig. 1. In the case of neon, a weak shock is formed in the weakly absorbing gas and a clean shock front is observed. The xenon profile also exhibits a well formed, sharp shock front; however, we also observe significant ionization of gas ahead of the shock front. This indicates

an ionization precursor formed by radiation emitted from the hot plasma and deposited in the otherwise undisturbed ambient gas. Further evidence of the radiative source of the precursor is found by comparing the xenon data with that from argon. The data suggest that there is little if any precursor in argon which we attribute to less efficient radiation production due to the lower  $Z$ .

We have used similar images to track the trajectories of blast waves in Ne, Ar, and Xe, data which are shown in Fig. 2. As expected, these data indicate a power law behavior. A least squares fit of functions of the form  $R = \beta t^\alpha$  was performed to these data to extract the deceleration parameter  $\alpha = Vt/R$ . To avoid a significant effect of the finite initial radius of the blast wave, the fits were performed for times beyond the time at which the blast wave radius exceeded twice the initial radius (roughly  $>7$  ns in most cases). The blast waves in both neon and argon exhibit trajectories with  $\alpha$  near 0.5, characteristic of an energy conserving, Sedov-Taylor blast wave. The deceleration parameter for xenon, however, was found to be lower than 0.5, where  $\alpha = 0.43 (\pm 0.010)$  until  $\sim 30$  ns. This indicates that the Xe blast waves do indeed begin to enter the radiative regime.

To help interpret the xenon data we have compared our results with simulations conducted with the radiation hydrodynamics code, HYADES [14]. HYADES is a one-dimensional Lagrangian hydrocode which treats radiation transport in the flux-limited multigroup diffusion approximation. Opacities were generated in-line using a screened-hydrogenic average-atom model assuming local thermodynamic equilibrium. The equation of state was taken from the SESAME library. To simulate the complex laser energy deposition, energy was deposited at  $t = 0$  in a region of the gas with a radius equal to the initial focal spot radius  $\sim 25 \mu\text{m}$ . The amount of energy was adjusted to fit the late time trajectory of the blast wave, which is not particularly sensitive to the early time details. A value of 8 mJ/mm provided a good fit and is close to the measured value of  $\sim 10$  mJ/mm. The predicted trajectory for Xe is compared with the experiment in Fig. 3(a). The very close agreement with the experimentally measured trajectory indicates that HYADES reproduces the experimentally inferred deceleration parameters.

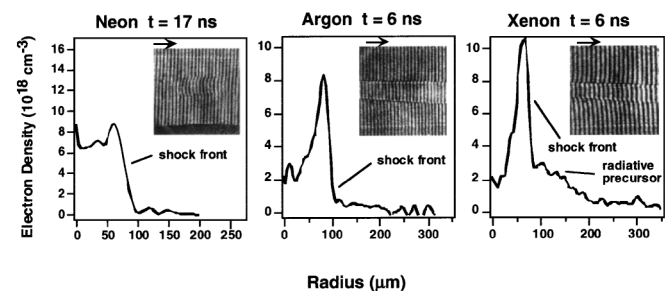


FIG. 1. Measured electron density profiles at one time of blast waves in Ne, Ar, and Xe. Interferograms from which these profiles were extracted are shown as insets.

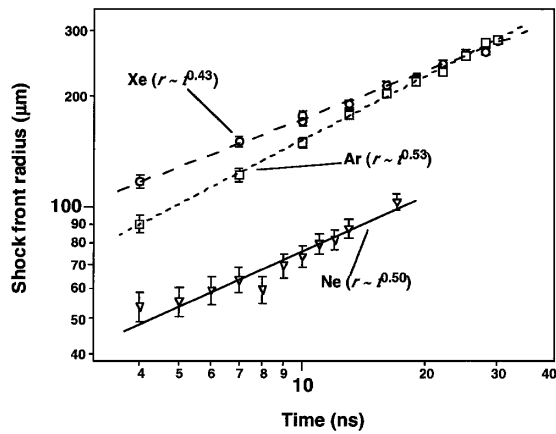


FIG. 2. Measured blast wave radius as a function of time for blast waves in Ne, Ar, and Xe. Best fit for the deceleration parameter is also shown.

At early time  $\leq 1$  ns before the shock wave has formed, the expansion of the plasma filament is governed by a supersonic electron thermal wave [15]. At very early time  $\leq 0.2$  ns the standard diffusion model for electron heat conduction in HYADES is not adequate because of the strongly nonlocal behavior of the electron transport. For this period we matched the data by adjusting the electron conduction coefficient, gradually returning it to the standard diffusion value by 0.2 ns. Although this is an *ad hoc* procedure we do not expect it to grossly affect the overall energetics of the blast wave many nanoseconds later, which is of most interest here. In fact, a calculation in which we limited the

early time electron conduction did not match the early time experimental data but resulted in the same conclusions for the later time blast wave propagation.

The extent to which radiative losses affect the simulated dynamics is illustrated in Fig. 3(b). Here the simulated blast wave internal energy per unit length and energy exiting the blast wave front as a function of time are shown. The blast wave loses a substantial fraction of energy via radiation during the first 30 ns of the wave evolution (50 mJ/cm by 30 ns, over 60% of the initial energy). Also plotted is the energy that leaves the entire system by radiation, defined as the energy exiting the simulation grid. The difference between this curve and the curve representing radiative loss from the blast wave shell indicates the amount of energy deposited in the ionization precursor. This implies that up to 20 mJ/cm (25% of deposited laser energy) gets deposited in the precursor at early time.

In this simulation, the predicted  $\alpha$  value is  $\sim 0.45$  around 10–20 ns and gradually climbs to the Sedov value of 0.5 near 50–60 ns. After this the value increases slightly as some of the radiated energy is recovered because energy deposited in the precursor at early time is swept up by the wave at later time. In order to eliminate the possibility that a departure from  $\alpha = 0.5$  behavior was due to memory of finite initial radius, a second simulation was conducted without radiation transport and took for its initial conditions those calculated at the time when the shock was beginning to form in the previous simulation. The calculation settled into  $\alpha = 0.5$  behavior by 7–10 ns, confirming that the departure from  $\alpha = 0.5$  behavior in the calculation shown in Fig. 3(a) results from radiative cooling effects.

The simulations present convincing evidence that the gross experimental blast wave dynamics are affected by radiative cooling. Despite this, however, we do not observe two important secondary phenomena: enhanced shell compression and development of thin shell instability. There are two reasons why enhanced shell compression is not observed. First, radiative preheating of the ambient gas to  $\sim 1$  eV reduces the Mach number from very high at room temperature ( $>30$ ) to a much smaller value ( $\sim 5$ ). This results in a reduction in compression from  $\sim 10$  ( $\gamma \sim 1.2$ ) in the strong shock limit for xenon to  $\sim 7$ . In addition, electron thermal conduction within the blast wave moves energy efficiently from the hot, low density core into the shocked gas raising its temperature so that the shell is thickened, and the predicted compression never actually exceeds  $\sim 4$ . We have demonstrated in a series of test calculations that, after the shock has formed, radiation loss from the hot core becomes increasingly less efficient as its density drops. Instead energy is conducted out of the core into the much denser shocked gas where it is efficiently radiated away. This mechanism is responsible for most of the continued radiative cooling of the blast wave long after the shock wave has formed and prevents density buildup that would otherwise occur behind a cooling shock wave.

Finally, we examined how this strong radiative cooling affected the blast wave stability. The presence of

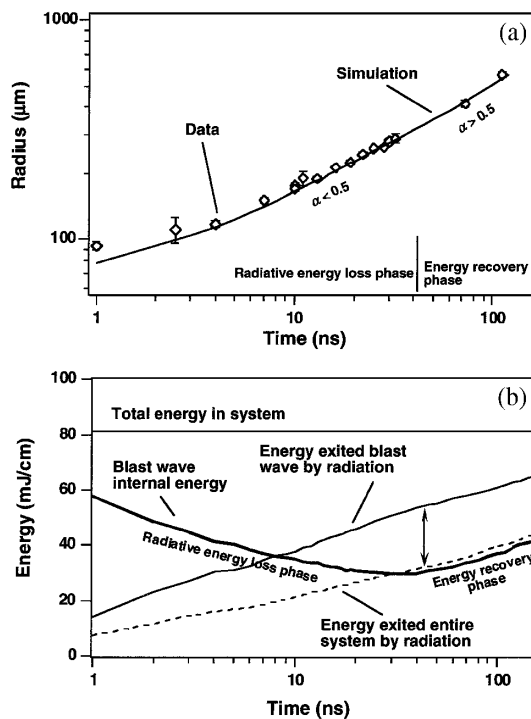


FIG. 3. (a) Plot of the Xe blast wave trajectory as a function of time found from both experiment and simulation. (b) Simulated dynamics of energy transport in the Xe blast wave.

instability growth was sought experimentally by conducting dark field imaging. We examined all gases in our experiments and none exhibited instability growth. Images of a Xe blast wave at times 4, 30, and 110 ns are shown in Fig. 4. The shock front is located at the thin bright region which appears extremely smooth down to the scale of the instrument resolution,  $\sim 10 \mu\text{m}$ , even at the latest time. This is in sharp contrast to observations made in Ref. [10].

To estimate growth rates of “sausagelike” perturbations on a cylindrical shell we have used an extension of Ott’s analysis [16] for thin shells including material accretion [17]. This model reproduces Vishniac’s result in the appropriate limit and has the advantage of carrying over into the nonlinear regime. The growth rate is given by  $\Gamma = \text{Re}[p(p - \rho v^2)/\sigma^2]^{1/4} k^{1/2}$ , where  $p$  is the pressure driving the shell,  $\rho v^2$  is the ram pressure of the ambient material on the shock,  $\sigma$  is the areal density of the shell, and  $k$  is the wave number of the perturbation. In the Sedov regime with  $\gamma \sim 1$  the growth rate reduces to  $(kp/2\sigma)^{1/2}$  since  $p \sim (1/2)\rho v^2$ . In the case of a strongly radiatively cooled wave,  $p \ll \rho v^2$  and the growth rate is reduced. HYADES predicts  $p \sim (1/6)\rho v^2$  and we obtain a growth factor  $[\exp(\int \Gamma dt)]$ , integrated from 10 to 100 ns] of  $\sim 20$  for a wavelength of  $100 \mu\text{m}$ , which is roughly  $\frac{1}{2}$  the value that would be obtained for an energy conserving Sedov wave. The instability model is strictly valid only for  $\lambda \gg \Delta R$ , and we regard the growth at  $\lambda = 100 \mu\text{m}$  to be an estimate of an upper bound on instability growth since the shell thickness  $\Delta R$  is  $\sim 30\text{--}50 \mu\text{m}$  while  $\Gamma \sim 1/\lambda$ . This suggests that the apparent absence of instability growth in the xenon blast waves results at least, in part, from the effective stabilizing influence of a relatively thick shell, which is itself a consequence of thermal conduction heating of the shocked gas, but also of the relatively low Mach number. However, further investigations will be required to establish this. Applying the same analysis to simulations of the experiments in Ref. [10] for spherical geometry we predict growth factors of  $\sim 100\text{--}1000$  for the shorter wavelengths which were observed to grow. The observations in Ref. [10] are therefore not inconsistent with the current work. This analysis will be expanded upon at a later date.

Thus, we can conclude that the production of blast waves entering the radiative regime is possible in ultrafast laser heated clustering gases under appropriate circumstances. We have experimentally observed the production of a radiation generated ionization precursor and have measured the increased deceleration predicted for strongly radiating shocks. Despite evidence of radiative cooling, neither enhanced shell compression nor thin shell instabilities were observed. The former is a consequence of shell heating due to thermal conduction from the hot core, reducing the

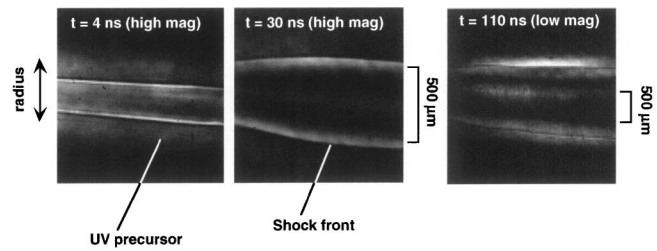


FIG. 4. Dark field images of the Xe blast wave at three different times.

compression and contributing to the lack of significant thin shell instability growth.

This work was performed under the auspices of the DOE, Contract No. W-7405-Eng-48. We acknowledge many useful conversations with R. P. Drake and the technical assistance of G. Hays, G. Anderson, V. Tsai, and R. Shuttlesworth.

\*Current address: Department of Physics, University of Texas, Austin, TX 78712.

- [1] C. F. McKee and B. T. Draine, *Science* **252**, 397 (1991).
- [2] J. M. Blondin, E. B. Wright, K. J. Borkowski, and S. P. Reynolds, *Astrophys. J.* **500**, 342 (1998).
- [3] N. Bartel *et al.*, *Science* **287**, 112 (2000).
- [4] J. M. Shull and C. F. McKee, *Astrophys. J.* **227**, 131 (1979).
- [5] R. I. Klein and D. T. Woods, *Astrophys. J.* **497**, 777 (1998).
- [6] Y. B. Zel’dovich and Y. P. Raizer, *Physics of Shock Waves and High-Temperature Hydrodynamic Phenomena* (Academic Press, New York, 1967).
- [7] E. T. Vishniac, *Astrophys. J.* **274**, 152 (1983).
- [8] D. Ryutov, R. P. Drake, J. Kane, E. Liang, B. A. Remington, and W. M. Wood-Vasey, *Astrophys. J.* **518**, 821 (1999).
- [9] J. C. Bozier, G. Thiell, J. P. L. Breton, S. Azra, M. Decroisette, and D. Schirmann, *Phys. Rev. Lett.* **57**, 1304 (1986).
- [10] J. Grun, J. Stamper, C. Manka, J. Resnick, R. Burris, J. Crawford, and B. H. Ripin, *Phys. Rev. Lett.* **66**, 2738 (1991).
- [11] T. Ditmire, K. Shigemori, B. A. Remington, K. Estabrook, and R. A. Smith, *Astrophys. J. Suppl.* **127**, 299 (2000).
- [12] T. Ditmire, R. A. Smith, J. W. G. Tisch, and M. H. R. Hutchinson, *Phys. Rev. Lett.* **78**, 3121 (1997).
- [13] K. Shigemori *et al.*, *Astrophys. J. Lett.* **533**, L159 (2000).
- [14] J. T. Larsen and S. M. Lane, *J. Quant. Spectrosc. Radiat. Transfer* **51**, 179 (1994).
- [15] T. Ditmire, E. T. Gumbrell, R. A. Smith, A. Djaoui, and M. H. R. Hutchinson, *Phys. Rev. Lett.* **80**, 720 (1998).
- [16] E. Ott, *Phys. Rev. Lett.* **29**, 1429 (1972).
- [17] D. D. Ryutov, M. S. Derzon, and M. K. Matzen, *Rev. Mod. Phys.* **167**, 72 (2000).